P H Y S I C A L   R E V I E W   L E T T E R S

Electro-Optic Modulation of Single Photons

Pavel Kolchin,* Chinmay Belthangady, Shengwang Du, G. Y. Yin, and S. E. Harris

Edward L. Ginzton Laboratory, Stanford University, Stanford, California 94305, USA
(Received 5 June 2008; published 3 September 2008)

We use the Stokes photon of a biphoton pair to set the time origin for electro-optic modulation of the wave function of the anti-Stokes photon thereby allowing arbitrary phase and amplitude modulation. We demonstrate conditional single-photon wave functions composed of several pulses, or instead, having Gaussian or exponential shapes.

This Letter demonstrates how single photons may be modulated so as to produce photon wave functions whose amplitude and phase are functions of time. The essential feature of this work is the use of one photon of a biphoton pair that is generated by spontaneous parametric down-conversion to establish the time origin for the modulation of the second photon. This is done by using electromagnetically induced transparency and slow light to produce time-energy entangled biphotons with pulse lengths of several hundred ns, and therefore, very long as compared to the temporal resolution of single-photon counting modules (about 40 ps). Once the time origin is established, the photon waveform may be modulated in the same manner as one modulates a classical pulse of light. For example, the single-photon waveform may be phase, frequency, amplitude, or even digitally modulated, with the maximum modulation frequency limited by the resolution of the detection of the first photon.

As shown in Fig. 1, we use cw pump and coupling lasers to generate time-energy entangled pairs of Stokes and anti-Stokes photons that propagate in opposite directions and are collected in single mode fibers. The detection of a Stokes photon at D_1 sets the time origin for firing the function generator that drives the electro-optic modulator (EOM) that modulates the wave function of the anti-Stokes photon. This latter photon is incident on the beam splitter where it is detected by D_2 or D_3. As shown in the following, we generate single photons whose modulated waveform is two rectangular pulses, is Gaussian, or is a time-reversed exponential.

The method demonstrated in this Letter might be used to optimally load a single photon into an optical cavity [1], or instead, to study the transient response of atoms to different single-photon waveforms. In the context of light-matter interfaces, it may improve the efficiency of storage and retrieval of single photons in atomic ensembles [2]. For quantum information applications, both amplitude and phase modulators could be used to allow full control over the single-photon waveforms. For example, one could construct a single-photon waveform that is a train of identical pulses with information encoded into the relative phase difference between consecutive pulses [3].

The generation of single photons with controlled waveforms has been demonstrated earlier by using the techniques of cavity QED, i.e., by coupling a single trapped ion to a high Q cavity and using an acousto-optic modulator to shape a pumping laser that is tuned close to the resonant transition [4]. In related work, Rempe and colleagues use a single Rb atom, again in a high Q cavity to generate single photons [5]. The suggestions and experiments of the Lukin and Kimble groups [6,7] together with the cavity approach of Vuletic [8] as well as the rapidly expanding work in the category of quantum storage followed by single-photon generation [9–15] offer other techniques for generating conditional single-photons. More generally, the use of one photon of a correlated pair as a trigger for a conditional second photon is reviewed by Lounis and Orrit [16].
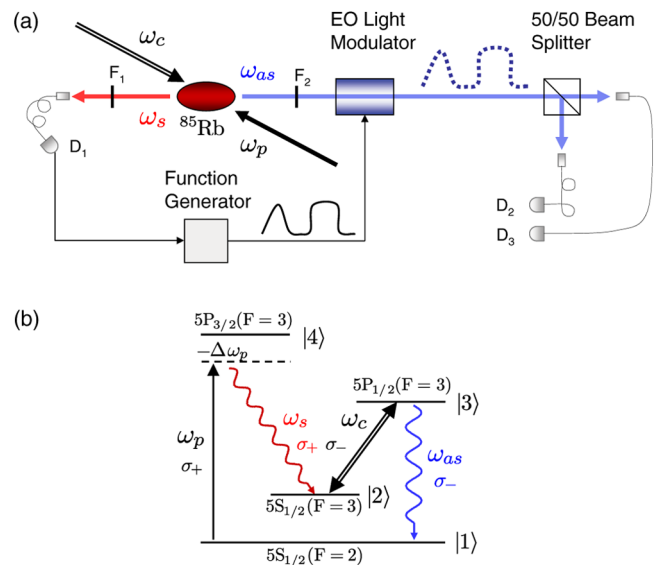

FIG. 1 (color online).   (a) Schematic of paired photon generation and conditional modulation. A Stokes photon detected by an SPCM sets the time origin for shaping the anti-Stokes photon with an electro-optic modulator. To within the accuracy of the SPCM, this allows shaping of both the amplitude and phase of the anti-Stokes photon. (b) Energy level diagram of ^{85}Rb for paired photon generation.

In this Letter, we use the technique of Balic *et al.* [17–19] to generate biphotons in a backward wave geometry where the length of the biphoton is determined by the slow group velocity associated with EIT. We first summarize the properties of this type of biphoton light source as recently developed by Du and colleagues [20]. This source uses a two-dimensional MOT with a cylindrical atomic cloud with a length of 1.7 cm, an aspect ratio of 25, and an estimated dephasing rate of the nonallowed $|1\rangle \rightarrow |2\rangle$ transition of $\gamma_{12} = 0.01\Gamma_3$, where $\Gamma_3 = 6$ MHz is the spontaneous decay rate out of the state $|3\rangle$. This source may be run at an optical depth in the range of 10 to 60 resulting in group velocities at the anti-Stokes wavelength of 3×10^5 to 2×10^4 m/s. This allows the generation of biphotons with temporal lengths that can be varied over the range of 50 to 900 ns and have estimated linewidths as small as 0.75 MHz. The generation rate of paired photons is about 2×10^5 pairs per second.

Figure 2 shows the coincidence count rate of detectors D_1 and D_2 without modulation at an optical depth of 40. In Fig. 2, the Rabi frequencies of the pump and coupling lasers are $\Omega_c = 2.2\Gamma_3$ and $\Omega_p = 0.59\Gamma_3$, and the detuning of the pump from resonance, $\Delta\omega_p = 24.4\Gamma_3$. With τ as the relative delay between Stokes and anti-Stokes detection times t_1 and t_2, respectively, and T_b as the bin width, the Glauber correlation function is related to the coincidence rate, $R_c(\tau)$ by $G^{(2)}(\tau) = R_c(\tau)/T_b$. This correlation function may, in turn, be expressed in terms of the square of the absolute value of the biphoton wave function $\Psi(t_1, t_1 + \tau)$ and the rate of generation of Stokes (R_s) and anti-Stokes (R_{as}) photons as $G^{(2)}(\tau) = |\Psi(t_1, t_1 + \tau)|^2 + R_s R_{as}$ [18].

Two features of the correlation function in Fig. 2 are: a mean width that is equal to the group delay time, as caused by EIT, of the anti-Stokes photon relative to the Stokes photon, and a sharp leading edge spike. This spike is a
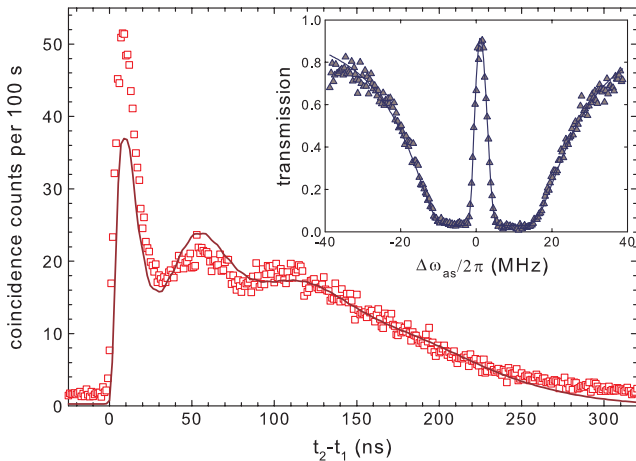

FIG. 2 (color online). No modulation; D_1-D_2 coincidence counts in a 1 ns bin as a function of the relative delay at an optical depth of 40. The inset shows the EIT transmission profile for the anti-Stokes photon (see text for further detail).

Sommerfeld-Brillouin precursor and has an approximate width that is equal to the opacity width of the EIT profile in the optically thick medium [21–23]. Figure 2 also shows the theoretically computed correlation function. Except at the peak of the precursor, the correlation shapes that are predicted by theory [17,18] and those that are observed experimentally are in good agreement. This agreement is important because it distinguishes the biphoton wave function from background counts which may also be modulated.

In order to account for experimental factors, the theoretical curve is multiplied by a factor of $\eta = 8.8 \times 10^{-4}$. This scaling factor takes into account the 10% duty cycle, 57% transmission at the beam splitter port, additional losses of about 20% in the beam splitter, Stokes and anti-Stokes filters efficiencies of 48% and 42%, respectively, fiber to fiber coupling of 75%, a detector efficiency of 50%, and EO light modulator insertion loss of 50%.

The discrepancy between theory and experiment that was reported in earlier publications [17,24] has been corrected. The greatly improved performance of the present source is due to the nonmetal geometry and the configuration of the 2D MOT, which taken together, have reduced the dephasing rate of the nonallowed transition by a factor of 30. Under optimum experimental conditions, the maximum ratio of paired counts to Stokes counts is 11%. With losses backed out, this corresponds to 73% as compared to the theoretical value of 75%.

The electro-optic amplitude modulator consists of phase modulators in both arms of a Mach-Zehnder (MZ) interferometer [25]. The degree of phase control in both arms depends on the type of the modulator. We use a z-cut modulator that requires $V_\pi = 1.75$ volts to cause the π phase shift required to go from minimum to maximum transmission and can be operated at a maximum frequency of 10 GHz. One port of the output beam splitter of the MZ interferometer is terminated so that the portion of the photon wave function that is not transmitted is lost. In general, if a Stokes photon is detected at time t_1, and the modulator is activated conditioned on this detection, then in the Heisenberg picture, the anti-Stokes operator at the output of the modulator is related to the input operator by $\hat{a}_{out}(t_2) = \int g(t_2, t_2')\hat{a}_{in}(t_2')dt_2'$. If there are no dispersive elements, then to within an unimportant phase factor, we may write $\hat{a}_{out}(t_2) = m(\tau)\hat{a}_{in}(t_2)$. The correlation function in the presence of the modulator is related to that in the absence of the modulator by

$$G_m^{(2)}(\tau) = |m(\tau)|^2 G^{(2)}(\tau). \tag{1}$$

With the biphoton wave function given by $\Psi(t_1, t_1 + \tau)$, the modulated (conditional) single-photon wave function is $m(\tau)\Psi(t_1, t_1 + \tau)$. We adjust the bias voltage at the input of modulator so that the output of the modulator $m(\tau)$ is related to the input voltage $V(\tau)$ by $m(\tau) = \sin[\phi(\tau)] \times \exp[i\alpha\phi(\tau)]$, where $\phi(\tau) = \pi V(\tau)/(2V_\pi)$, and α is a

phase modulation parameter. For a z-cut amplitude modulator as used here, $\alpha = 0.75$. This phase shift may be eliminated by using an x-cut modulator.

In somewhat more detail, the detection of a Stokes photon by detector D_1 (Perkin-Elmer SPCM-AQR-13) triggers both the start input of a time-to-digital converter (FAST Comtec TDC 7886S) as well as a function generator (Agilent 33250A-80MHz) which generates the desired modulation signal. The function generator along with auxiliary logic gates has an electronic delay of about 190 ns. To partially compensate for this delay, the anti-Stokes photon is optically delayed by 140 ns using a 30 m long single mode polarization maintaining fiber. The anti-Stokes beam is then passed through the EO modulator (EOSPACE Inc.) driven by the output of the function generator. Verification of the single-photon nature of the modulated anti-Stokes photon is done using a 50-50 beam splitter and detectors D_2 and D_3, which are connected to the stop inputs of the time-to-digital converter. Coincidence counts are binned into histograms with 1 ns bin width and plotted as a function of the difference between the arrival times of the Stokes and anti-Stokes photons.

We use two rectangular pulses as the modulation signal. Figure 3(a) shows coincidence counts between detectors D_1 and D_2 with and without modulation. In the latter case, the EO light modulator is set to maximum transmission. Of importance, there is no vertical scaling between the modulated and nonmodulated waveforms. Coincidence histograms between detectors D_1 and D_3 (not shown) have similar shapes. In Fig. 3(b), we show modulated photons with two different waveforms. In the first case, we drive the modulator with a Gaussian pulse. In the second case, we design the function generator output waveform so as to compensate for the functional (or nonlinear) distortion in such a way that the output of the modulator is an exact rising exponential. The solid lines show theoretical curves which are calculated by using the scope traces of the output voltage of the function generator as $V(\tau)$.

In the presence of the modulator, we define the retrieval efficiency as the probability to generate a single anti-Stokes photon on the condition that the paired Stokes photon is detected, $\mathcal{E}_R = R_p/R_s$. Here, R_p is the total paired rate, calculated from the area under the correlation curves, measured at detectors D_1, D_2 and D_1, D_3, minus the uncorrelated background floor. When the modulator is fully open [Fig. 2], we measure $\mathcal{E}_R = 3.5\%$. When losses at the beam splitter, modulator, filters, fiber-to-fiber coupling, and detector efficiency in the anti-Stokes path are backed out, this corresponds to a retrieval efficiency of 55%. With the modulator present, the retrieval efficiency is waveform dependent. For the examples of two square pulses, rising exponential and Gaussian waveforms, the retrieval efficiency is $\mathcal{E}_R = 1.3$, 0.61, and 0.9%, respectively. If no losses were present, these efficiencies would be 21, 9.4, and 11.2%.
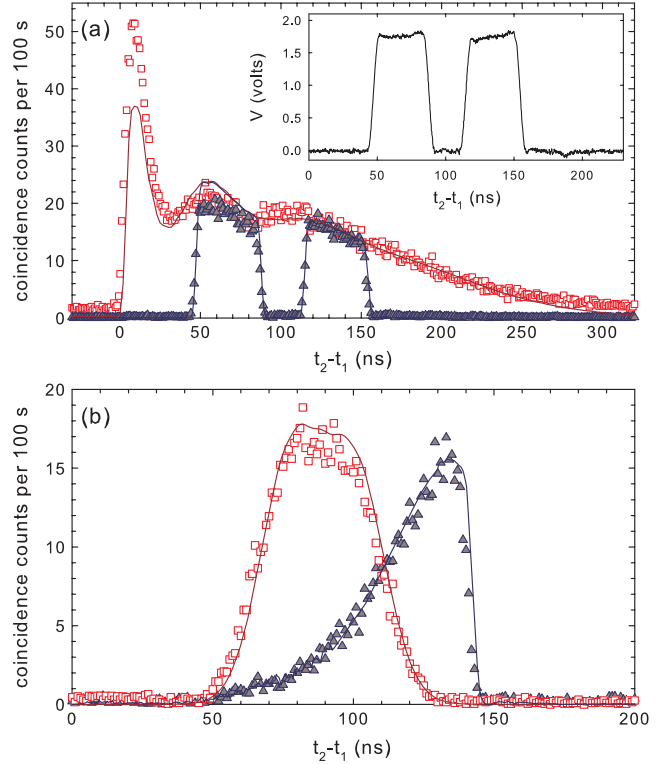

FIG. 3 (color online). D_1-D_2 coincidence counts in a 1 ns bin as a function of the delay between Stokes and anti-Stokes photons. (a) Modulated ($\triangle$) and unmodulated ($\square$) waveforms. (b) Waveforms with Gaussian ($\square$) and rising exponential ($\triangle$) shapes. The experimental data ($\square$, $\triangle$) were collected over 2000 s. The solid curves for cases (a) and (b) are plotted from theory. The inset in part (a) is the scope trace of the output voltage of the function generator.

Since single photons incident on a beam splitter must go into one output port or the other, in the ideal case where there are no two-photon events and there is no excess scattered light, we would expect no threefold coincidences at the detectors. A measure of the quality of heralded single photons that quantifies suppression of two-photon events is given by the conditional correlation function [26],

$$g_{\mathrm{cond}}^{(2)}(0) = \frac{N_{123}N_1}{N_{12}N_{13}}. \tag{2}$$

Here, N_1 is the number of the Stokes counts at D_1, N_{12}, and N_{13} are the number of twofold coincidence counts within a time window T_c at detectors D_1, D_2 and D_1, D_3; and N_{123} is the number of threefold coincidence counts within this same time window.

In Fig. 4, triangles and squares show measured $g_{\mathrm{cond}}^{(2)}(0)$ versus Stokes rate with and without modulation. The modulation is done with the same signal as in Fig. 3(a). We set T_c equal to the nominal length of the unmodulated biphoton (285 ns). At a Stokes rate of $2.2 \times 10^4\ \mathrm{sec}^{-1}$ which corresponds to $\Omega_p = 0.26\Gamma_3$, we obtain $g_{\mathrm{cond}}^{(2)}(0) = 0.2 \pm 0.04$
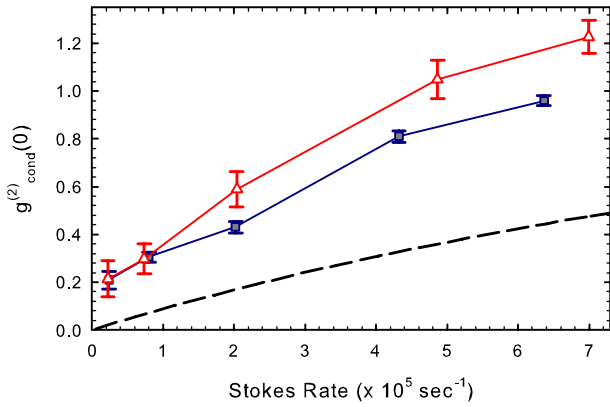
FIG. 4 (color online). Conditional threefold correlation function $g_{\text{cond}}^{(2)}(0)$ as a function of the Stokes rate for unmodulated ($\square$) and modulated ($\triangle$) single-photon generation. The dashed curve shows the theoretical limit for $g_{\text{cond}}^{(2)}(0)$ in the absence of excess light scattering (see text).

and $g_{\text{cond}}^{(2)}(0) = 0.21 \pm 0.07$ for the unmodulated and modulated waveforms, respectively. The fact that the measured $g_{\text{cond}}^{(2)}(0)$ is less than 0.5, (the limiting value for a two-photon Fock state), is indicative of the near-single-photon character of the light source.

Because there is a small probability for the parametric down-conversion process to generate multiple pairs of biphotons, even in the absence of spurious light scattering, the conditional correlation function is not zero. The dashed curve in Fig. 4 shows the theoretical prediction for the conditional correlation function that results from such multiple scattering events. Because of light scattering from both the pump and coupling lasers, the experimental curves lie above this limiting value.

We describe two control experiments: In the first, we remove the 30 m long optical fiber so as to modulate the uncorrelated background noise in the tail of the correlation function. Here, we measure $g_{\text{cond}}^{(2)}(0) = 1.2$. In the second experiment, we apply modulation at random times, using an external 10 MHz digital signal as a trigger for the function generator. As expected, we observe a reduced rate of paired counts and no change in the shape of the correlation function.

This Letter has demonstrated a technique for using one photon of a biphoton pair to set the time origin and to trigger an electro-optic modulator to shape the waveform of the second photon. The importance of the electro-optic method is its speed and ability to modulate phase as well as amplitude. The technique provides the technology for studying the response of atoms to shaped single-photon waveforms on a time scale comparable to the natural linewidth.

The authors acknowledge helpful discussions with I. A. Khan, G. J. Milburn, S. Sensarn, and A. E. Siegman. The work was supported by the U.S. Air Force Office of Scientific Research, the U.S. Army Research Office, and the Defense Advanced Research Projects Agency.

*pkolchin@stanford.edu
[1] J. I. Cirac *et al.*, Phys. Rev. Lett. **78**, 3221 (1997).
[2] A. Gorshkov *et al.*, Phys. Rev. Lett. **98**, 123601 (2007); I. Novikova *et al.*, Phys. Rev. Lett. **98**, 243602 (2007); N. B. Phillips *et al.*, Phys. Rev. A **78**, 023801 (2008); I. Novikova *et al.*, arXiv:0805.1927v1 [Phys. Rev. A (to be published)].
[3] K. Inoue *et al.*, Phys. Rev. Lett. **89**, 037902 (2002).
[4] M. Keller *et al.*, Nature (London) **431**, 1075 (2004).
[5] A. Kuhn *et al.*, Phys. Rev. Lett. **89**, 067901 (2002).
[6] C. H. van der wal *et al.*, Science **301**, 196 (2003).
[7] A. Kuzmich *et al.*, Nature (London) **423**, 731 (2003).
[8] J. K. Thompson *et al.*, Science **313**, 74 (2006).
[9] C. W. Chou *et al.*, Phys. Rev. Lett. **92**, 213601 (2004).
[10] M. D. Eisaman *et al.*, Phys. Rev. Lett. **93**, 233602 (2004).
[11] M. D. Eisaman *et al.*, Nature (London) **438**, 837 (2005).
[12] T. Chaneliere *et al.*, Nature (London) **438**, 833 (2005).
[13] D. N. Matsukevich *et al.*, Phys. Rev. Lett. **97**, 013601 (2006).
[14] J. Laurat *et al.*, Opt. Express **14**, 6912 (2006).
[15] S. Chen *et al.*, Phys. Rev. Lett. **97**, 173004 (2006).
[16] B. Lounis *et al.*, Rep. Prog. Phys. **68**, 1129 (2005).
[17] V. Balić *et al.*, Phys. Rev. Lett. **94**, 183601 (2005).
[18] P. Kolchin, Phys. Rev. A **75**, 033814 (2007).
[19] C. H. R. Ooi *et al.*, Phys. Rev. A **75**, 013820 (2007).
[20] S. Du *et al.*, Phys. Rev. Lett. **100**, 183603 (2008).
[21] H. Jeong *et al.*, Phys. Rev. Lett. **96**, 143901 (2006).
[22] F. J. Lynch *et al.*, Phys. Rev. **120**, 513 (1960).
[23] S. Du *et al.*, "Observation of Optical Precursors at the Biphoton Level," Opt. Lett. (to be published).
[24] P. Kolchin *et al.*, Phys. Rev. Lett. **97**, 113602 (2006).
[25] Keang-Po Ho, *Phase-Modulated Optical Communication Systems* (Springer, New York, 2005).
[26] P. Grangier, G. Roger, and A. Aspect, Europhys. Lett. **1**, 173 (1986).